Highly Enantioselective 6π Photoelectrocyclizations Engineered by Hydrogen-Bonding

Wesley B. Swords,^{1,‡} Hanna Lee,^{2,3,‡} Yerin Park,^{2,3} Franco Llamas,¹ Kazimer L. Skubi,^{1,4} Jiyong Park,^{3,2} Ilia A. Guzei,¹ Mu-Hyun Baik,^{3,2,*} Tehshik P. Yoon^{1,*}.

¹Department of Chemistry, University of Wisconsin–Madison, 1101 University Avenue, Madison, Wisconsin 53706, United States. Email: tyoon@chem.wisc.edu

²Department of Chemistry, Korea Advanced Institute of Science and Technology (KAIST), Daejeon 34141, Republic of Korea. Email: mbaik2805@kaist.ac.kr

³Center for Catalytic Hydrocarbon Functionalizations, Institute for Basic Science (IBS), Daejeon 34141, Republic of Korea. Email: mbaik2805@kaist.ac.kr

⁴Department of Chemistry, Carleton College, Northfield, Minnesota 55057, United States

[†]These authors contributed equally to this work.

ABSTRACT: Photochemical electrocyclization reactions are valued both for their ability to produce structurally complex molecules and their central role in elucidating fundamental mechanistic principles of photochemistry. We present herein a highly enantioselective 6π photoelectrocyclization catalyzed by a chiral Ir(III) photosensitizer. This transformation was successfully realized by engineering a strong hydrogen-bonding interaction between a pyrazole moiety on the catalyst and a basic imidazolyl ketone on the substrate. To shed light on the origin of stereoinduction, we conducted a comprehensive investigation combining experimental and computational mechanistic studies. Results from density functional theory (DFT) calculations underscore the crucial role played by the prochirality and the torquoselectivity in the electrocyclization process, as well as the steric demand in the subsequent [1,4]-H shift step. Our findings not only offer valuable guidance for developing chiral photocatalysts but also serve as a significant reference for achieving high levels of enantioselectivity in the 6π photoelectrocyclization reaction.

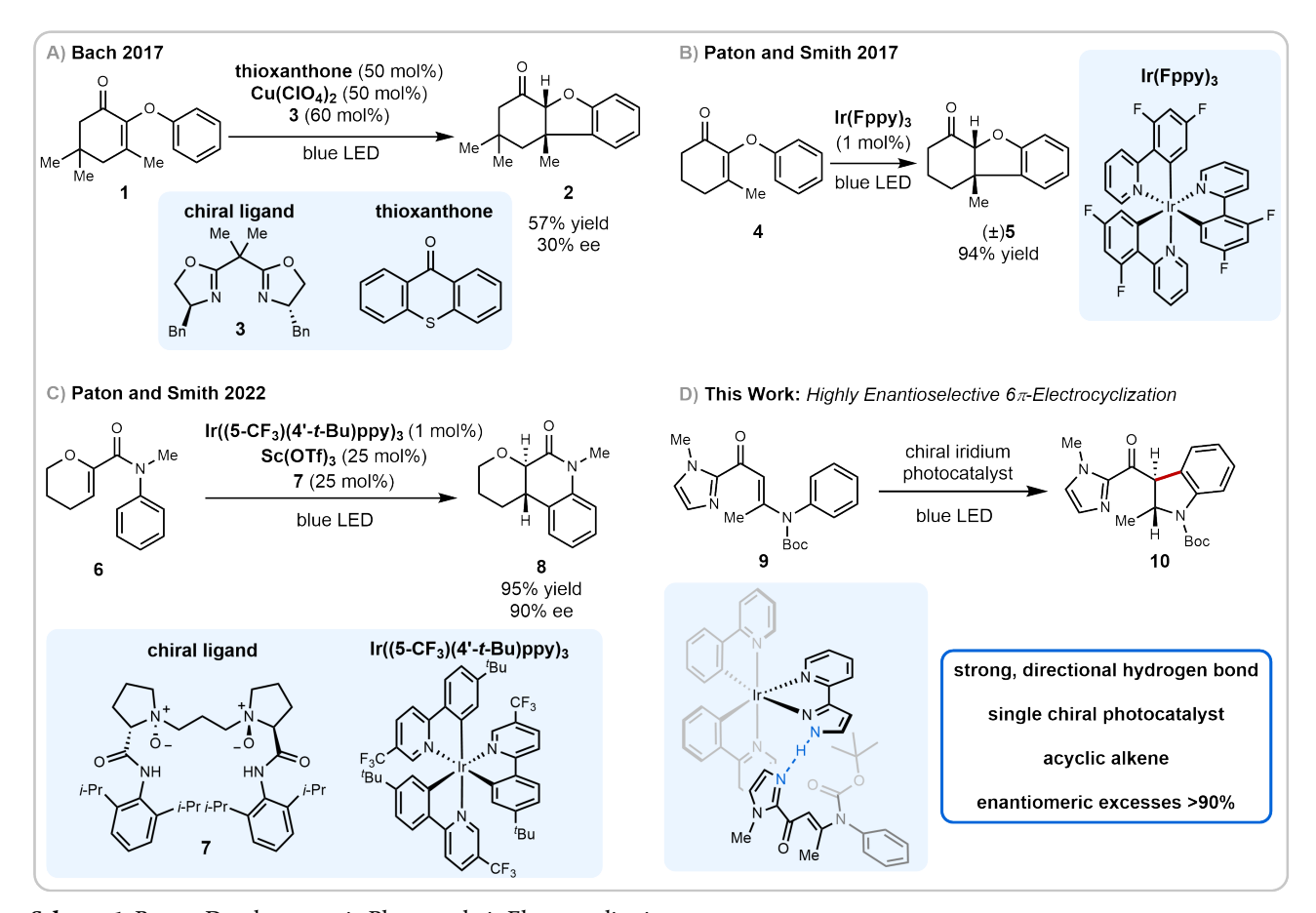
Introduction

Electrocyclizations constitute a class of pericyclic reactions of both fundamental and practical significance in organic chemistry. Because they can assemble complex cyclic scaffolds from simpler, more synthetically accessible linear precursors, these reactions have found application as key ring-forming steps in total synthesis.[1] More fundamentally, the complementary torquoselectivity of thermal and photochemical electrocyclizations constitutes a canonical demonstration of the consequences of orbital symmetry in pericyclic reactions. While a variety of methods for asymmetric catalysis of thermally initiated electrocyclizations have been described, [2] highly enantioselective photoelectrocyclization reactions have proven more difficult to develop, [3] consistent with the general challenge of controlling the high reactivity of electronically excited organic intermediates. Generally effective strategies for asymmetric catalysis of excited-state photoreactions have only begun to emerge over the past decade; [4] However, these new strategies have focused primarily on developing cycloaddition reactions.^[5] New methods to conduct catalytic photoelectrocyclization reactions with high enantiocontrol thus provide a significant new capacity in asymmetric synthesis.

Three seminal publications by Bach demonstrate the challenge of conducting enantioselective catalytic electrocyclization reactions. In 2003, Bach reported the first example of an enantioselective 6π photoelectrocyclization in 57% ee, but the chiral hydrogen-bonding template had no catalytic effect and had to be used at 2 equiv for

optimal ee. [3e] Subsequently, Bach reported a dual-catalyst system comprising a chiral Cu(II) Lewis acid and a thioxanthone sensitizer for 6π photoelectrocyclization of 2-aryloxycyclohexenones up to 47% ee (Scheme 1A). [6] Finally, the same group reported the design of a chiral thiourea—thioxanthone hybrid catalyst that could perform the same transformation in 12% ee. [7] Ir-polypyridyl photosensitizers often show superior efficiency over organic photosensitizers for similar applications. Recently, Paton and Smith demonstrated that α -aryloxycyclohexenones undergo efficient racemic photoelectrocyclization to afford dihydrobenzofurans in the presence of an Ir(Fppy)₃ photosensitizer (Scheme 1B). [8] During the preparation of this manuscript, the same authors reported that the combination of a chiral Lewis acid with an Ir photosensitizer could affect the enantioselective electrocyclization of diverse acetanilides in up to 90% ee (Scheme 1C). [9]

We have recently reported that enantiopure chiral Ir(III) complexes functionalized with hydrogen-bonding pyridyl-pyrazole ligands are efficient triplet-energy chiral photocatalysts for highly enantioselective [2+2] photocycloaddition reactions. [10] We hypothesized that this catalyst design should be applicable to any triplet photoreaction catalyzed by structurally analogous Ir(III) polypyridyl photocatalysts, including 6π photoelectrocyclization reactions. Preliminary attempts to utilize this hydrogen-bonding chiral Ir(III) photosensitizers in the asymmetric electrocyclization of the α -aryloxycyclohexenones studied by Paton and Smith (4), however,



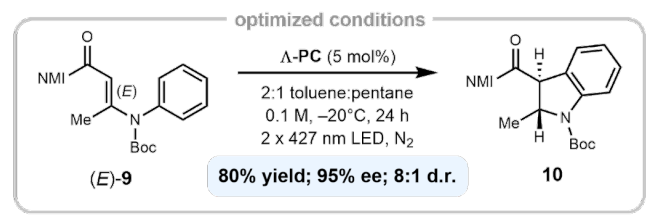
Scheme 1. Recent Developments in Photocatalytic Electrocyclizations.

failed to deliver synthetically useful enantioenrichment. We reasoned that one important difference from our previous, successful investigations might be the hydrogen-bonding ability of the substrate. Previously, our studies focused on quinolone-derived substrates capable of two-point hydrogen-bonding with the pyrazole moiety;^[10] the oxygen functionalities of 4, however, have low Brønsted basicity and thus seem less likely to participate in a similarly well-organized hydrogen-bonding network. We speculated, therefore, that introducing a more Brønsted basic binding domain into the substrate might provide a better-ordered catalyst-substrate assembly that could result in higher ee's. C-Acylimidazoles seemed particularly promising in this regard. Various asymmetric methods, including asymmetric photochemical reactions, utilize imidazoles as strong catalyst-binding auxiliary groups that are readily cleaved from the enantioenriched products under mild conditions.[11] We have also recently reported a chiral Brønsted acid-catalyzed [2+2] photocycloaddition of C-acylimidazoles in which the substrate bound to the catalyst through a single-point hydrogen-bonding interaction involving the imidazolyl nitrogen.[12] We envisioned, therefore, that substrate 9 featuring a C-acylimidazole unit might also construct a well-defined hydrogen bond with a pyrazolyl N-H group on a chiral Ir(III) photocatalyst and engage in a 6π photoelectrocyclization with high enantioselectivity (Scheme 1D).

Results and Discussion

Under optimized conditions, chiral Ir(III) complex Λ -PC featuring a pyridyl-pyrazole ligand catalyzes the 6π photoelectrocyclization of $\bf 9$ in high diastereo- and enantioselectivity (Figure 1). The

design of 9 was inspired by pioneering studies by Chapman and others on the 6π photoelectrocyclization of *N*-aryl enamines. [13] Notably, the selectivity of the photoreaction was strongly influenced by the solvent polarity. While a non-polar solvent mixture of 2:1 toluene:pentane proved to be ideal, higher-dielectric solvents such as CH₂Cl₂ and CH₃CN resulted in poorer ee's, consistent with the attenuated strength of hydrogen-bonding interactions in these solvents. The temperature was also an important factor for optimal stereoselectivity. Conducting the reaction at -20 °C instead of room temperature resulted in a significant increase in ee; however, further lowering of the reaction temperature to -40 °C did not significantly improve the ee and resulted in a slight loss of diastereoselectivity. Lowering the photocatalyst concentration (1 mol%) or reaction concentration (0.01 M) reduced both the yield and ee (entries 6 and 7). Performing the reaction under air instead of an inert atmosphere resulted in a consumption of 9, but the low yield of product was indicative of oxygen-mediated decomposition (entry 8). Control reactions showed both light and the photocatalyst were required for a productive reaction (entries 9 and 10). Finally, the carbamate linking group appears to be required: amine- and ether-linked substrates did not undergo productive electrocyclization (11 and 13). We reasoned that the diminished reactivities are due to the inefficient substrate sensitization. Indeed, the calculated triplet energies of 11 and 13 were 53.4 kcal/mol and 54.0 kcal/mol, respectively, that are 3~4 kcal/mol higher than that of 9, which was 50.9 kcal/mol. The finding manifested the importance of triplet energy matching between the photosensitizer and the substrate. We also note N-methyl linking group (12) resulted in a degradation, which was in line with the



deconstruction —				
entry	deviation from optimal	yield ^a	d.r. ^b	eec
1	toluene	57%	6:1	87%
2	CH_2Cl_2	29%	3:1	87%
3	CH ₃ CN	17%	3:1	53%
4	20 °C	60%	8:1	73%
5	−40 °C	58%	5:1	96%
6	1 mol% Λ-PC	39%	5:1	74%
7	$0.01~\mathrm{M}$	55%	7:1	82%
8	air instead of N2	<5% ^d	-	_
9	dark	0%e	_	_
10	no Λ-PC	0%e	_	-
11	(Z)-9 ^f	84%	8:1	91%
13	11 (NH) instead of 9	0% ^e	_	-
14	12 (NMe) instead of 9	0% ^d	_	-
15	13 (O) instead of 9	0% ^e	_	_
Me NMI	F ₃ C N N N N N N N N N N N N N N N N N N N	NMI	11: X = N 12: X = N 13: X = O	Ме

Figure 1. Optimization studies for photocatalytic 6π electrocyclization.^a Yield determined from the crude reaction versus an internal standard. ^b d.r. determined from the unpurified reaction mixture. ^c ee determined via chiral HPLC. ^d Significant degradation occurred. ^e >95% returned starting material based on crude NMR. ^f 6:1 (Z):(E) ratio.

previous observation that the 6π photocyclized tertiary N-alkyl products are unstable. [13e]

Studies probing the scope of the reaction under optimized conditions are summarized in Scheme 2. The carbamate protecting group could be varied with only minor effects on yield and enantioselectivity, and the diastereomeric ratio improved using larger Boc and Fmoc carbamates (10, 14, 15). Substitution about the aniline group was reasonably tolerated; methyl substitution at the p-position (16) conserved the high enantioselectivity, though with a decreased 45% yield. A p-fluorine (17) drastically decreased the rate of the reaction, albeit with good mass recovery, while the d.r. and enantiomeric excess (ee) remained high. In contrast, substitution at the *m*-position was highly successful with both 3- (18-20) and 3,5-anilines (21, 22) providing high yields and enantioselectivity. The 3-Ph-substituted substrate cyclized to produce 18 in 86% yield of two regioisomers (1.1:1), slightly favoring the 4-substituted product. Chlorine (19) and bromine (20) were tolerated in the 3-position favoring the 4substituted indolines in 2.5 and 2:1 regioisomeric ratios and impressive 96% and 97% ees, respectively. The structure of 20 was unambiguously confirmed via single-crystal X-ray diffraction. The favored regioisomers agree with previous racemic reports of similar electrocyclizations. [8] For the disubstituted products, the 3,5-dimethylaniline-derived substrate underwent cyclization to $\boldsymbol{21}$ in 76% yield and a nearly equal ratio of diastereomers with high ee (93% and 96%, see SI for minor ee's). The 3,5-dibromoaniline substrate, in comparison, reacted to give $\boldsymbol{22}$ in high yield (70%) with a >10:1 d.r. and in 96% ee. Finally, modification of the β -alkyl substituent had little effect on the yield and enantioselectivity (23 and 24). A slightly more complex substrate modified with both a cyclohexyl group and a 3,5-dichloroaniline underwent electrocyclization giving $\boldsymbol{25}$ in 50%

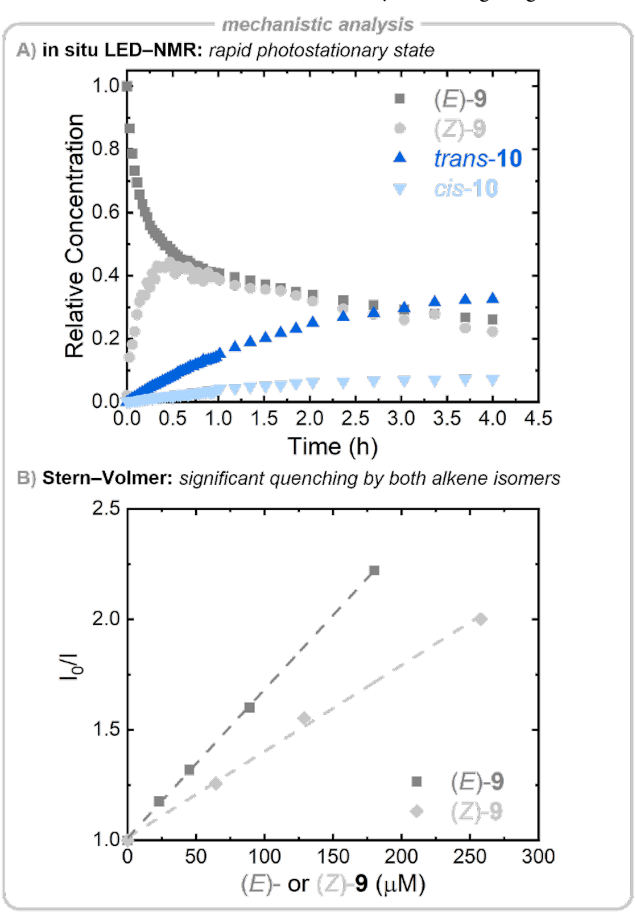
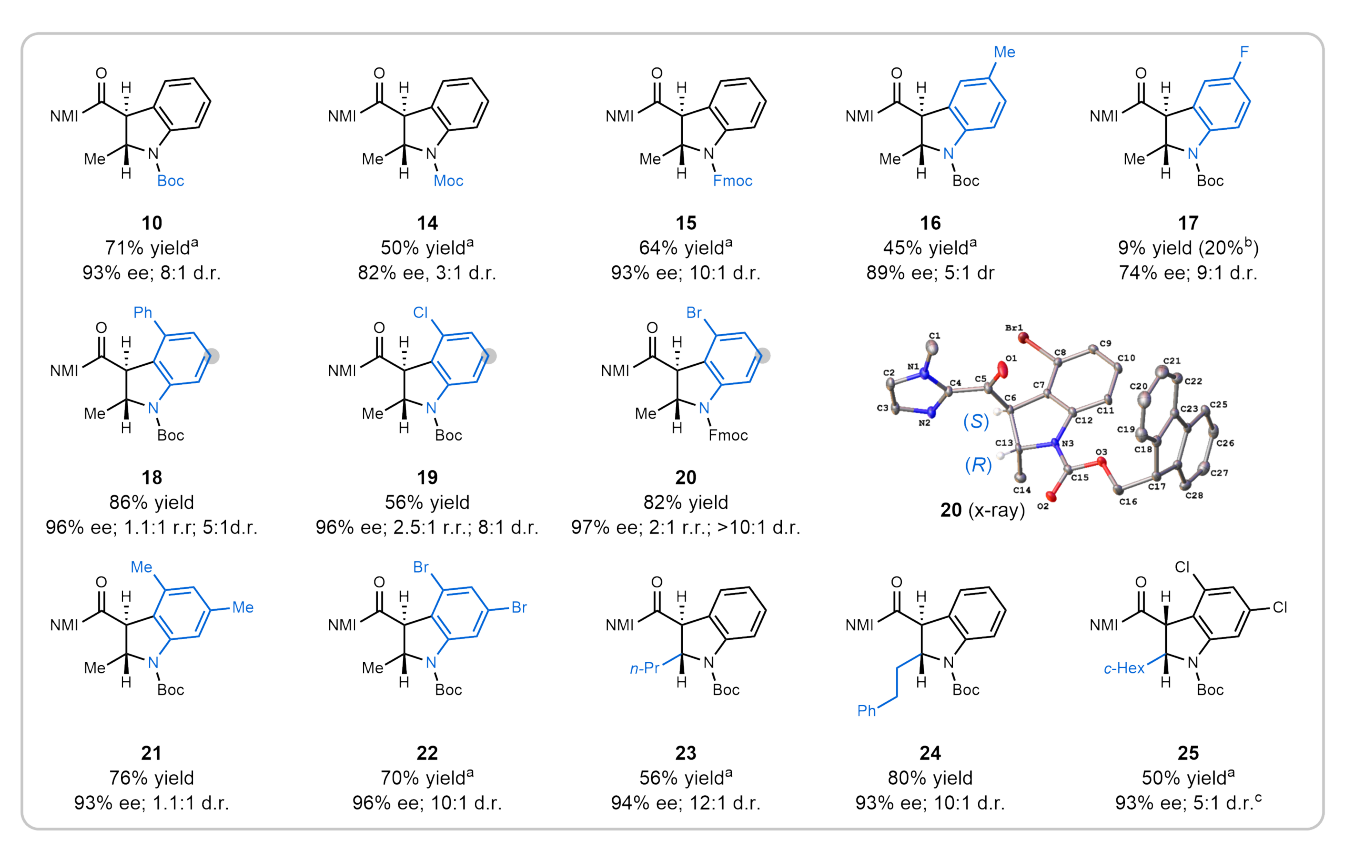


Figure 2. A) Reaction profile tracking of the two substrate isomers, (E)-and (Z)-9, and the two product isomers, trans- and cis-10. B) Stern-Volmer analysis of the quenching of the excited-state photocatalyst by the two substrate isomers.

yield and 93% ee. Surprisingly, in this case, the *cis* diastereomer was the major product by a 5:1 ratio. Compounds highlighting some of the limitations of this reaction are provided in the supplemental information.

To obtain insight into the mechanism, we first monitored the reaction progress at ambient temperature using LED–NMR (Figure 2A). [14] Geometrically pure (E)-9 undergoes rapid photoisomerization and achieves a photostationary 1:1 E:Z ratio within 30 min. Product-forming electrocyclization is significantly slower, resulting in a 6:1 ratio of diastereomeric indolines. These results are consistent with the expectation that both alkene isomerization and electrocyclization proceed through a common triplet-state intermediate. They also suggest a Curtin–Hammett scenario in which triplet sensitization of both alkene isomers is fast but that the partitioning of the triplet diradical intermediate towards electrocyclization is relatively inefficient. Consistent with this hypothesis, UV-Vis titration



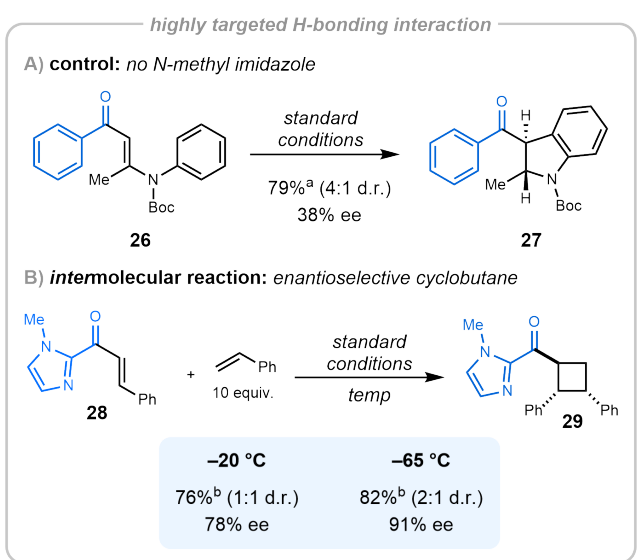
Scheme 2. Enantioselective Photoelectrocyclization Scope. Conditions: 0.15 mmol scale, 0.1 M starting material, 2:1 toluene:pentane, –20 °C, 2×427 nm Kessil® LEDs, 24 h. Diastereomer ratios (d.r.) were determined by ¹H nuclear magnetic resonance (¹H NMR) analysis of the unpurified reaction mixture. Grey dot notes minor regioisomer. Enantiomeric excesses (ee) were determined using chiral high-performance liquid chromatography (HPLC) and are reported for the major regio- or diastereomer. ¹ Isolated yield of the major diastereomer. ¹ H NMR yield. ¹ The *cis*-product was isolated as the major diastereomer.

studies showed that both geometric isomers of **9** bind readily to the photocatalyst with similar association constants ($K_{EQ,E} = 2,200$ and $K_{EQ,Z} = 1,200$). Similarly, a Stern–Volmer analysis further showed that both isomers quench the excited state of ${}^{3}\mathbf{\Lambda}$ -**PC** with similar efficiencies (Figure 2B, $K_{SV,E} = 6,700 \,\mathrm{M}^{-1}$ and $K_{SV,Z} = 3,900 \,\mathrm{M}^{-1}$).

An energy transfer pathway for both E:Z isomerization and electrocyclization was supported by electrochemical experiments. The chiral Ir photocatalyst (Λ -PC) exhibited irreversible oxidation (+1.68 V vs. SCE) and reduction (-1.42 V vs. SCE) waves by cyclic voltammetry. Using the estimated triplet energy of the photocatalyst (60.2 kcal/mol), we calculated the excited-state reduction potentials of the photocatalyst to be (Ir^{III*/II}) = +1.23 V vs. SCE and (Ir^{IV/III*}) = -0.93 V. Neither can access the reduction (<-1.82 V) or oxidation (+1.39 V) potentials of the substrate, ruling out the possibility of a photoredox mechanism.

The strong hydrogen-bonding interaction provided by the *C*-acylimidazole functional handle appears to be critical for the success of this enantioselective reaction. Replacing the imidazole with a phenyl ring resulted in a drastically reduced 38% ee while maintaining a similar yield and diastereomeric ratio (27, Scheme 3A). This result implies that although the photocatalyst's pyrazole N–H bond can recruit a substrate by hydrogen bonding to other polar functional groups in the substrate (presumably the carbamate), the basic imidazole moiety results in a stronger, more well-ordered catalyst–substrate assembly that provides superior stereocontrol. As a test of the generality of this interaction, we examined the intermoecular [2+2] cycloaddition of imidazolyl enone 28^[12] using the conditions

optimized for the intramolecular electrocyclization. This experiment provided cyclobutane **29** in high yield, equimolar diastereoselectivity (*trans-syn* vs. *trans-trans*) and promising enantioselectivity (78% ee) (Scheme 3B). Lowering the reaction temperature to –65

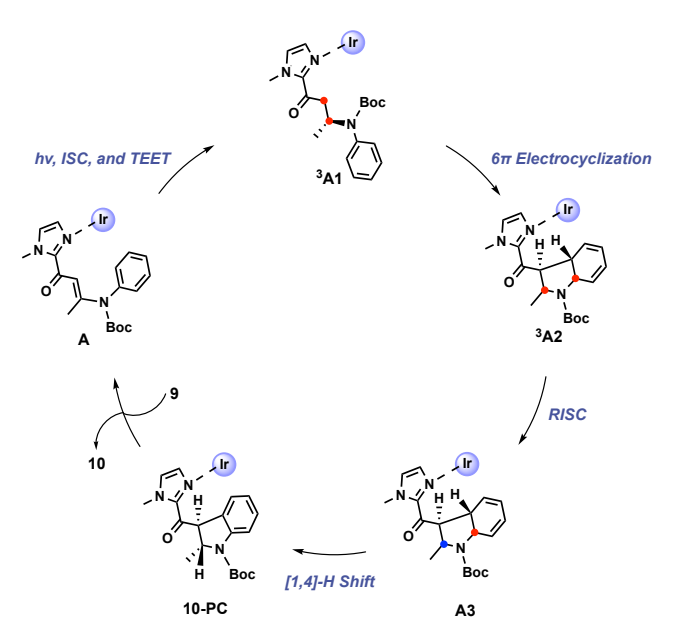


Scheme 3. Electrocyclization of a phenyl ketone substrate and an enantioselective intermolecular [2+2] cycloaddition. ^a Only the yield of the isolated major diastereomer is reported. ^b Yield is of both diastereomers isolated together.

°C improved the yield, diastereoselectivity, and enantioselectivity, providing *trans-syn* **29** in 82% yield, 2:1 d.r., and 91% ee. Together, these data suggest that the hydrogen-bonding interaction between the imidazolyl nitrogen and the photocatalyst results in a well-organized assembly that will enable the same chiral photocatalyst to be used for a range of mechanistically dissimilar inter- and intramolecular reactions with only minimal adjustment of the reaction parameters.

The proposed catalytic cycle leading to the major product 10 is described in Scheme 4. Initially, an encounter complex, labeled as $\bf A$, is formed between photocatalyst $\bf \Lambda$ -PC and substrate 9. The key factor in this complexation is the hydrogen-bonding between the imidazolyl nitrogen of 9 and the pyrazole group of $\bf \Lambda$ -PC. Upon photoexcitation of the encounter complex, a rapid intersystem crossing (ISC) occurs, leading to the formation of the triplet excited state, ${}^3\bf{A1}$, through triplet excited-state energy transfer (TEET). Subsequently, a 6π electrocyclization takes place, resulting in the formation of ${}^3\bf{A2}$. Reverse intersystem crossing (RISC) and a suprafacial [1,4]-H shift yields the hydrogen-bonded complex 10-PC. Ultimately, product 10 is displaced by 9, resetting the catalytic cycle.

Figure 3 illustrates the results of our computational mechanistic investigations aimed at better understanding the origin of enantiose-lectivity. To start, substrate **9** may form four different hydrogen-bonded encounter complexes with Λ -**PC**, denoted as **A1**, **B1**, **C1**, and **D1**. These complexes ultimately give rise to the (S,R), (S,S), (R,S), and (R,R) stereoisomers of **10**, respectively. The photoexcited substrates within the encounter complexes undergo two consecutive photochemical reactions: i) 6π electrocyclization and ii) [1,4]-H shift. The Woodward-Hoffmann rules suggest that the 6π electrocyclization should proceed in a conrotatory fashion. [8,14] This conrotatory motion of the π -orbitals and the orientation of the approaching phenyl group jointly contribute to the formation of four



Scheme 4. Catalytic cycle of 6π photoelectrocyclizations. TEET = Triplet energy transfer. Ir = Λ -PC, Boc = *tert*-butyloxycarbonyl group.

viable intermediates 3 **A2**, 3 **B2**, 3 **C2**, and 3 **D2**. While there are eight conrotatory transition states possible in the excited electronic manifold, four of them are favored due to reduced steric interaction between the aryl group of **9** and ppy ligand of **\Lambda-PC**. Moving forward, a lower steric demand in the *si*-face attack, compared to the *re*-face counterpart, results in two distinct outcomes, 3 **A2** and 3 **B2**, which lead to the formation of (S,R) and (S,S) stereoisomers, respectively. In the subsequent suprafacial [1,4]-H shift, the presence of more conducive non-covalent interactions between the catalyst and

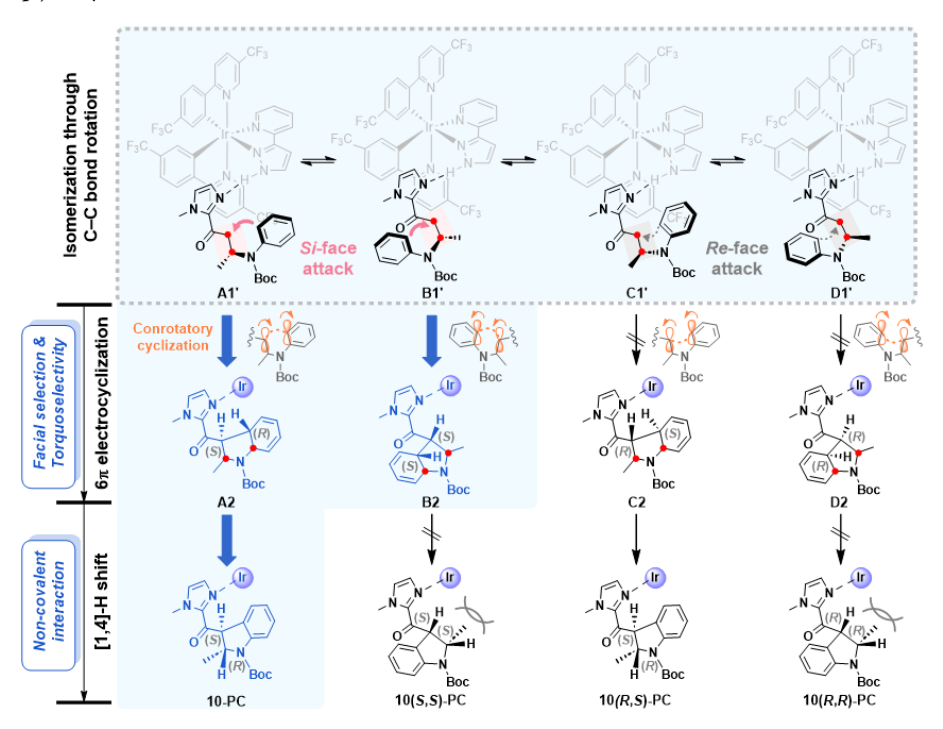


Figure 3. Stereodetermining factors: facial selection, torquoselectivity, and non-covalent interaction. The major stereoisomer **10** can be obtained by the *si*-face attack of the phenyl carbon to the α -carbon and conrotatory 6π electrocyclization followed by ISC and [1,4]-H shift.

substrate in 3 **A2** drives the formation of the major product **10**, bearing the (S_{i} R) configuration.

The detailed mechanism of photocatalytic 6π electrocyclization has been explored in detail using density functional theory (DFT) calculations. Special attention was given to the possible structures of the hydrogen-bonded encounter complexes that can be formed between **9** and Λ -PC. We found that there are two encounter complexes, denoted as **A** and **B**, wherein the imidazole nitrogen of **9** serves as the hydrogen-bond acceptor to interact with Λ -PC (Figure 4). As an alternative, we considered the possibility of hydrogen-bond formation at the carbonyl moiety of **9**, giving rise to two additional encounter complexes, termed **A'** and **B'** (Figure S16). Our

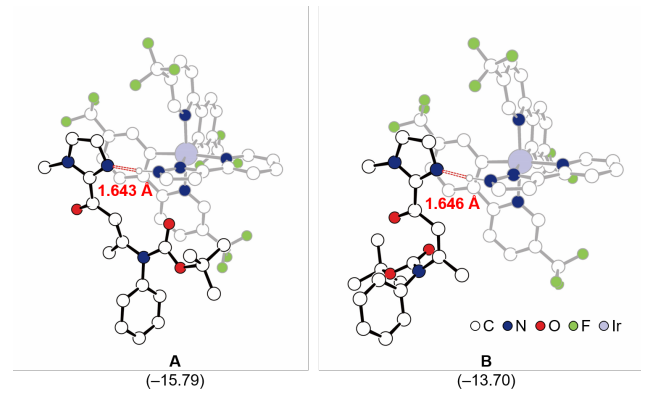


Figure 4. Two viable encounter complexes, **A** and **B**, consisting of Λ **-PC** and **9**. The Gibbs free energy of each complex is shown in kcal/mol in parentheses. Hydrogen bonds and their lengths are expressed in red. Hydrogens attached to carbons omitted for clarity.

DFT calculations revealed that **A** and **B** exhibit lower energy states compared to **A'** and **B'**. Notably, **A** emerged as the lowest energy

complex, boasting a 2.1 kcal/mol advantage over B, primarily attributable to favorable non-covalent interactions between the phenylpyridine ligand of Λ -PC and substrate 9. In complex A, the double bond of the α,β-unsaturated carbonyl assumes an anti-configuration, whereas in complex B, it adopts a syn-configuration. Interestingly, the other two conformers (A' and B'), wherein hydrogen bonding occurs via the carbonyl on 9, were found to be energetically less favorable by more than 3.3 kcal/mol (Figure S16). The disparities in Gibbs free energy strongly suggest that A' and B' represent species that are 700 to 15000 times less populated than A. This observation underscores the fact that the imidazole nitrogen functions as a stronger hydrogen-bonding acceptor when compared to the carbonyl oxygen - correlation consistent with the relative Brønsted basicity of these two sites. Importantly, the computed Gibbs free binding energies for ${\bf A}$ and ${\bf B}$ are -15.8 and -13.7 kcal/mol, respectively, implying that their dissociation constants (K_D) are within the subpicomolar range. This level of stability ensures that the substrate-catalyst complexes can withstand subsequent photoexcitation and bond-forming processes.

Figure 5 shows the energy profile of the 6π electrocyclization process starting from **A**. Our computational analysis confirms that the bond formation via the *si*-face attack leads to the formation product **10** with an (S,R) configuration at the newly formed sp³ carbon centers, consistent with the experimental results. The reaction sequence begins with photoexcitation, followed by intersystem crossing (ISC), and intermolecular TEET from **A-PC** to **9**. This prepares the triplet excited species 3 **A1**, where the α and β carbons of the carbonyl group in **9** exhibit diradical character (Figure S17). Subsequently, a C–N bond rotation generates 3 **A1**, which then engages the phenyl group of **9** for the *si*-face attack on the photoexcited double bond. The 6π electrocyclization leads to the formation of 3 **A2**, which includes a newly formed N-heterocyclic 5-membered ring. This

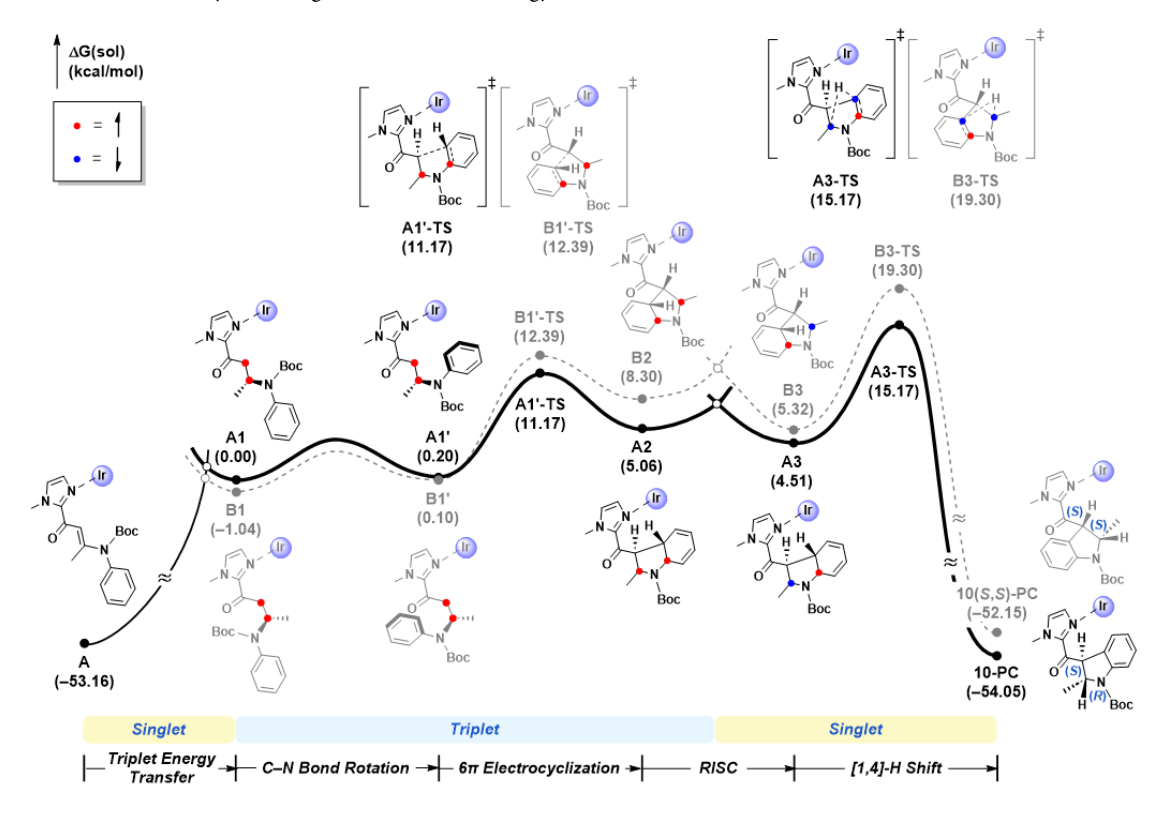


Figure 5. Reaction energy profile for the formation of **10-PC** and **10(S,S)-PC** products. Ir = Λ -**PC**, Boc = *tert*-butyloxycarbonyl group.

transition proceeds through a conrotatory transition state ${}^3A1'$ -TS, with a computed activation energy of 11.2 kcal/mol relative to 3A1 . This observation aligns with the well-known preference for conrotatory products in 6π electrocyclization reactions. Following this, reverse intersystem crossing (RISC) occurs, converting the triplet diradical species 3A2 to a singlet counterpart A3. The [1,4]-H shift follows, passing through the transition state A3-TS, with an activation energy of 15.2 kcal/mol, which is likely the slowest step among the photochemical processes. This step involves the migration of a hydrogen atom from the phenyl ring to the β -carbon of the carbonyl group, thereby restoring the aromaticity of the substrate. Importantly, the suprafacial [1,4]-H shift preserves the chirality of the intermediate. Finally, the product is released, yielding 10 with (S_iR) configuration.

We also explored the mechanistic pathway leading to the minor diastereomer, 10(S,S). After photoexcitation, intermediate ${}^{3}B1'$ is formed as the phenyl group of the substrate aligns itself toward the si-face attack on the photoexcited double bond. It is noteworthy that prochiral intermediates exist in equilibrium within the triplet manifold: ³B1' can be reached either through the C-N bond rotation from ³B1 or the C-C bond rotation from ³A1', with computed energy barriers of 14.1 and 7.8 kcal/mol, respectively (Figure S18). The conrotatory motion of π -lobes in ${}^{3}\mathbf{B1}'$ leads to ${}^{3}\mathbf{B2}$, traversing the transition state 3B1'-TS with an activation barrier of 12.4 kcal/mol. Finally, RISC and [1,4]-H shift afford the minor product 10(S,S), passing through the transition state B3-TS with a computed barrier of 19.3 kcal/mol. In contrast to the formation of 10 and 10(S,S), the production of the other two diastereomers 10(R,S)and 10(R,R), which involve the 6π electrocyclization with a *re*-face attack of the phenyl group, is predicted to be significantly slower due to their higher activation energies. Mechanistic details for these diastereomers are presented in Figure S19, highlighting that the activation energies of the 6π electrocyclization steps, ${}^{3}C1'$ -TS and ${}^{3}D1'$ -TS, are computed to be 18.5 and 22.2 kcal/mol, respectively. These values are notably higher than those of ³A1'-TS and ³B1'-TS. Consequently, we concluded that the difficulty encountered in the initial 6π electrocyclization steps, attributed to the higher steric demand between the phenyl group of $\bf 9$ and the ppy ligand of $\bf \Lambda$ -PC, hinders the re-face attack.

Our computational analysis revealed that the [1,4]-H shift is most likely the rate-determining step for the major product 10. This step is crucial as it not only restores the aromaticity of the product but also preserves the chirality of the newly formed sp^3 carbons. Our insights into this process were further enhanced through distortion-interaction analysis and depictions of non-covalent interactions, as illustrated in Figures S20 and S21. In essence, the favorable interaction between the substrate and photocatalyst serves to reduce the activation barrier associated with the [1,4]-H shift, ultimately leading to the formation of the major product 10. We note that the intermediates leading up to the [1,4]-H shift are in equilibrium, given that the activation energies of all preceding steps are lower than that of the hydrogen atom shift.

Conclusion

We have developed a highly enantioselective 6π photoelectrocyclization reaction using a single chiral Ir(III) photosensitizer. Through the strategic engineering of a strong hydrogen-bonding interaction between the pyrazole moiety on the chiral photocatalyst Λ -**PC** and the imidazolyl ketone in the substrate **9**, we achieved indoline products with good yields and remarkably high enantiomeric

excesses (>90%). Our comprehensive experimental and computational investigations provide valuable insights into the mechanistic intricacies of this process. Notably, we delineate the dual functionality of the Λ -PC as a triplet sensitizer and hydrogen-bonding donor. The formation of robust hydrogen bonded encounter complexes plays a pivotal role in enabling the highly enantioselective 6π photoelectrocyclization, highlighting the importance of substrate-catalyst interactions in stereocontrol. Furthermore, through detailed DFT calculations, we revealed the precise mechanism of the photocatalytic cycle and the factors driving high stereoselectivity. Steric demands lead to a preferential si-face attack, while torquoselectivity in the excited state manifold ensures the conrotatory 6π electrocyclization. Non-covalent interactions between the catalyst and substrate govern the diastereoselectivity during the [1,4]-H shift step. These findings provide crucial guidance for developing chiral photocatalysts and open new avenues for achieving highly enantioselective 6π photoelectrocyclization reactions.

ASSOCIATED CONTENT

Supporting Information

The Supporting Information is available free of charge on the ACS Publications website.

Experimental procedures, characterization data, spectra for all new compounds, crystallographic data, Cartesian coordinates of all computed structures, and binding studies (PDF)

Crystallographic data for **A-PC** (CIF) Crystallographic data for (E)-9 (CIF) Crystallographic data for **20** (CIF)

AUTHOR INFORMATION

Corresponding Authors

Tehshik P. Yoon – Department of Chemistry, University of Wisconsin–Madison, 1101 University Avenue, Madison, Wisconsin 53706, United States; orcid.org/0000-0002-3934-4973; Email: tyoon@chem.wisc.edu

Mu-Hyun Baik – Center for Catalytic Hydrocarbon Functionalizations, Institute for Basic Science (IBS), Daejeon 34141, Korea; Department of Chemistry, Korea Advanced Institute of Science and Technology (KAIST), Daejeon 34141, Korea; orcid.org/0000-0002-8832-8187; Email: mbaik2805@kaist.ac.kr

ACKNOWLEDGMENT

Funding for this project was provided by the NSF (CHE-1954262). W.B.S. acknowledges an NIH Kirschstein-NRSA Postdoctoral Fellowship (F32GM134611). NMR and MS facilities at UW–Madison are funded by the NIH (1S10 OD020022-1) and a generous gift from the Paul J. and Margaret M. Bender Fund. Bruker Quazar APEX2 was purchased by the UW–Madison Department of Chemistry through a generous gift from Paul J. and Margaret M. Bender. The purchase of the Bruker D8 VENTURE Photon III X-ray diffractometer was partially funded by the NSF (CHE-1919350). We thank Kyana M. Sanders (UW-Madison) for her assistance with structural studies. The Bruker Avance III 600 NMR spectrometer and LED components were supported by the NIH (S10 OD012245). We also thank the Institute for Basic Science in Korea for financial support (IBS-R010-A1).

REFERENCES

- [1] a) Beaudry, C. M.; Malerich, J. P.; Trauner, D. Biosynthetic and Biomimetic Electrocyclizations. *Chem. Rev.* **2005**, 105, 4757–4778. b) Bian, M.; Li, L.; Ding, H. Recent Advances on the Application of Electrocyclic Reactions in Complex Natural Product Synthesis. *Synthesis*, **2017**, 49, 4383–4413.
- [2] a) Thompson, S.; Coyne, A. G.; Knipe, P. C.; Smith, M. D. Asymmetric Electrocyclic Reactions. *Chem. Soc. Rev.* **2011**, *40*, 4217–4231. b) Sleet, C. E.; Tambar, U. K.; Maity, P. Brønsted acid catalyzed enantioselective pericyclic reactions. *Tetrahedron* **2017**, *73*, 4023–4038.
- [3] a) Ramamurthy, V. Achiral Zeolites as Reaction Media for Chiral Photochemistry. *Molecules* **2019**, *24*, 3570. b) Naito, T.; Tada, Y.; Ninomiya, I. Asymmetric Photocyclization of N- α , β -Unsaturated Acylanilides. *Heterocycles* **1984**, *22*, 237–240. c) Formentín, P.; Sabater, M. J.; Chretíen, M. N.; Garçia, H.; Scaiano, J. C. Enantioselective photocyclization of p-toluidides of α , β -unsaturated carboxylic acids in solution. A mechanistic and preparative study. *J. Chem. Soc., Perkin Trans.* **2002**, *2*, 164–167. d) Bach, T.; Bergmann, H.; Harms, K. Enantioselective Photochemical Reactions of 2-Pyridones in Solution. *Org. Lett.* **2001**, *3*, 601–603. e) Bach, T.; Grosch, B.; Strassner, T.; Herdtweck, E. Enantioselective [6 α]-Photocyclization Reaction of an Acrylanilide Mediated by a Chiral Host. Interplay between Enantioselective Ring Closure and Enantioselective Protonation. *J. Org. Chem.* **2003**, *68*, 1107–1116.
- [4] a) Genzink, M. J.; Kidd, J. B.; Swords, W. B.; Yoon, T. P. Chiral Photocatalyst Structures in Asymmetric Photochemical Synthesis. *Chem. Rev.* **2022**, *122*, 1654–1716. b) Prentice, C.; Morrisson, J.; Smith, A. D.; Zysman-Colman, E. *Beilstein J. Org. Chem.* **2020**, *16*, 2363–2441.
- [5] a) Poplata, S.; Tröster, A.; Zou, Y.-Q.; Bach, T. Recent Advances in the Synthesis of Cyclobutanes by Olefin [2+2] Photocycloaddition Reactions, *Chem. Rev.* **2016**, *116*, 9748–9815. b) Sherbrook, E. M.; Yoon, T. P. Asymmetric Catalysis of Triplet-State Photoreactions. In *Specialist Periodical Reports: Photochemistry*; Albini, A., Protti, S., Eds.; Royal Society of Chemistry: Croydon, UK, 2019; Vol. 46, pp 432–448. c) Ramamurthy, V.; Sivaguru, J. Supramolecular Photochemistry as a Potential Synthetic Tool: Photocycloaddition. *Chem. Rev.* **2016**, *116*, 9914–9993.
- [6] Edtmüller, V.; Pöthig, A.; Bach, T. Enantioselective photocyclisation reactions of 2-aryloxycyclohex-2-enones mediated by a chiral copper-bisox-azoline complex. *Tetrahedron* **2017**, *73*, 5038–5047.
- [7] Mayr, F.; Mohr, L.-M.; Rodriguez, E.; Bach, T. Synthesis of Chiral Thiourea-Thioxanthone Hybrids. *Synthesis* **2017**, *49*, 5238–5250.
- [8] Münster, N.; Parker, N. A.; van Dijk, L.; Paton, R. S.; Smith, M. D. Visible Light Photocatalysis of 6π Heterocyclization. *Angew. Chem. Int. Ed.* **2017**, 56, 9468-9472.
- [9] Jones, B. A.; Solon, P.; Popescu, M. V.; Du, J.-Y.; Paton, R. S.; Smith, M. D. Catalytic Enantioselective 6π Photocyclization of Acrylanilides. *J. Am. Chem. Soc.* **2023**, *145*, 171–178.
- [10] a) Skubi, K. L.; Kidd, J. B.; Jung, H.; Guzei, I. A.; Baik, M. H.; Yoon, T. P. Enantioselective Excited-State Photoreactions Controlled by a Chiral Hydrogen-Bonding Iridium Sensitizer. *J. Am. Chem. Soc.* **2017**, *139*, 17186–

- 17192. b) Zheng, J.; Swords, W. B.; Jung, H.; Skubi, K. L.; Kidd, J. B.; Meyer, G. J.; Baik, M. H.; Yoon, T. P. Enantioselective Intermolecular Excited-State Photoreactions Using a Chiral Ir Triplet Sensitizer: Separating Association from Energy Transfer in Asymmetric Photocatalysis. *J. Am. Chem. Soc.* **2019**, *141*, 13625–13634.
- [11] a) Huang, X.; Meggers, E. Asymmetric Photocatalysis with Bis-cyclometalated Rhodium Complexes. *Acc. Chem. Res.* **2019**, *52*, 833–847. b) Tyson, E. L.; Farney, E. P.; Yoon, T. P. Photocatalytic [2+2] Cycloadditions of Enones with Cleavable Redox Auxiliaries. *Org. Lett.* **2012**, *14*, 1110–1113. c) Evans, D. A.; Song, H.-J.; Fandrick, K. R. Enantioselective Nitrone Cycloadditions of α,β -Unsaturated 2-Acyl Imidazoles Catalyzed by Bis (oxazolinyl) pyridine–Cerium (IV) Triflate Complexes. *Org. Lett.* **2006**, *8*, 3351–3354.
- [12] Sherbrook, E. M.; Genzink, M. J.; Park, B.; Guzei, I. A.; Baik, M.-H.; Yoon, T. P. Chiral Brønsted acid-controlled intermolecular asymmetric [2+2] photocycloadditions. *Nat. Commun.* **2021**, *12*, 5375.
- [13] a) Chapman, O. L.; Eian, G. L. Photochemical transformations. XXVIII. Photochemical synthesis of 2,3-dihydroindoles from N-aryl enamines. J. Am. Chem. Soc. 1968, 90, 5329-5330. b) Chapman, O. L.; Eian, G. L.; Bloom, A.; Clardy, J. Photochemical transormations. XXXVIII. Nonoxidative photocyclization of N-aryl enamines. A facile synthetic entry to trans-hexahydrocarbazoles. J. Am. Chem. Soc. 1971, 93, 2918-2928. c) Yamada, K.; Konakahara, T.; Ishihara, S.; Kanamori, H.; Itoh, T.; Kimura, K.; Iida, H. Photochemical reaction of enamino ketones. Tet. Lett. 1972, 13, 2513-2516. d) Ibrahim-Ouali, M.; Sinibaldi, M.-È.; Troin, Y.; Guillaume, D.; Gramain, J.-C. Diastereoselective photochemical synthesis of 3,3'-disubstituted indolines. Tetrahedron. 1997, 53, 16083-16096. e) Wu, C.-J.; Cao, W.-X.; Lei, T.; Li, Z.-H.; Meng, Q.-Y.; Yang, X.-L.; Chen, B.; Ramamurthy, V.; Tung, C.-H.; Wu, L.-Z. A sustainable synthesis of 2-aryl-3-carboxylate indolines from N-aryl enamines under visible light irradiation. Chem. Commun. **2017**, 53, 8320–8323. f) Modha, S. G.; Pöthig, A.; Dreuw, A.; Bach, T. $[6\pi]$ Photocyclization to cis-Hexahydrocarbazol-4-ones: Substrate Modification, Mechanism, and Scope. J. Org. Chem. 2019, 84, 1139-1153.
- [14] a) Nitschke, P.; Lokesh, N.; Gschwind, R. M. Combination of illumination and high-resolution NMR spectroscopy: Key features and practical aspects, photochemical applications, and new concepts. *Prog. Nucl. Magn. Reson. Spectrosc.* **2019**, *114–115*, 86–134. b) Ji, Y.; DiRocco, D. A.; Kind, J.; Thiele, C. M.; Gschwind, R. M.; Reibarkh, M. LED-Illuminated NMR Spectroscopy: A Practical Tool for Mechanistic Studies of Photochemical Reactions. *ChemPhotoChem* **2019**, *3*, 984–992. c) Skubi, K. L.; Swords, W. B.; Hofstetter, H.; Yoon, T. P. LED-NMR Monitoring of an Enantioselective Catalytic [2+2] Photocycloaddition. *ChemPhotoChem* **2020**, *4*, 685–690.
- [15] a) Hoffmann, R.; Woodward, R. B. Conservation of Orbital Symmetry. *Acc. Chem. Res.* **1968**, *1*, 17–22. b) Kirmse, W.; Rondan, N. G.; Houk, K. N. Stereoselective Substituent Effects on Conrotatory Electrocyclic Reactions of Cyclobutenes. *J. Am. Chem. Soc.* **1984**, *106*, 7989–7991.

Highly Enantioselective 6π -Electrocyclzation